

**Table S2. Relative evolutionary rate of enhancers in neuron related tissues, Related to Figure 1**

All enhancers		Neuron expressed enhancers			Neuronal-stem-cell expressed enhancers		
Branch	# of enhancers	# of enhancers	Relative evolutionary rate	p-value	# of enhancers	Relative evolutionary rate	p-value
<b>B4</b>	410	66	$4.03 = \frac{(66/410)}{(1,307/32,748)} \&$	$<10^{-16}$	47	$4.78 = \frac{(47/410)}{(785/32,748)} \&$	$7.9 \times 10^{-14}$
<b>B3</b>	330	23	1.75	0.009	21	2.65	0.04
<b>B2</b>	758	56	1.85	$4.5 \times 10^{-6}$	45	2.48	0.01
<b>B1</b>	3,103	197	1.59	$5.1 \times 10^{-10}$	99	1.33	0.03
<b>B0</b>	28,147	965	0.86	N/A	573	0.85	N/A
All branches	32,748 **\$	1,307 *	N/A	N/A	785 *	N/A	N/A

The relative evolutionary rate used to generate Figure 1C. &: Examples of the detailed calculation of relative evolutionary rate. The background control (dominators in &) was calculated using numbers of enhancers on all branches (B0...B4) marked with \*. P-values represent the statistically significant deviation from 1 (Chi-squared test). \$: the evolutionary age classification of all enhancers (n =32748) is provided in Table S1.

**Table S3. Analysis of covariance (ANCOVA) on the evolutionary rate of hEANTs, Related to Figure 1**

Parameter	ANCOVA p value
SNP density*	$1.6 \times 10^{-8}$
Enhancer length*	0.84
GC content*	$2.5 \times 10^{-6}$
Enhancer type	$<10^{-16}$

\*These factors were normalized into Z-scores before being used in the linear regression model of ANCOVA.

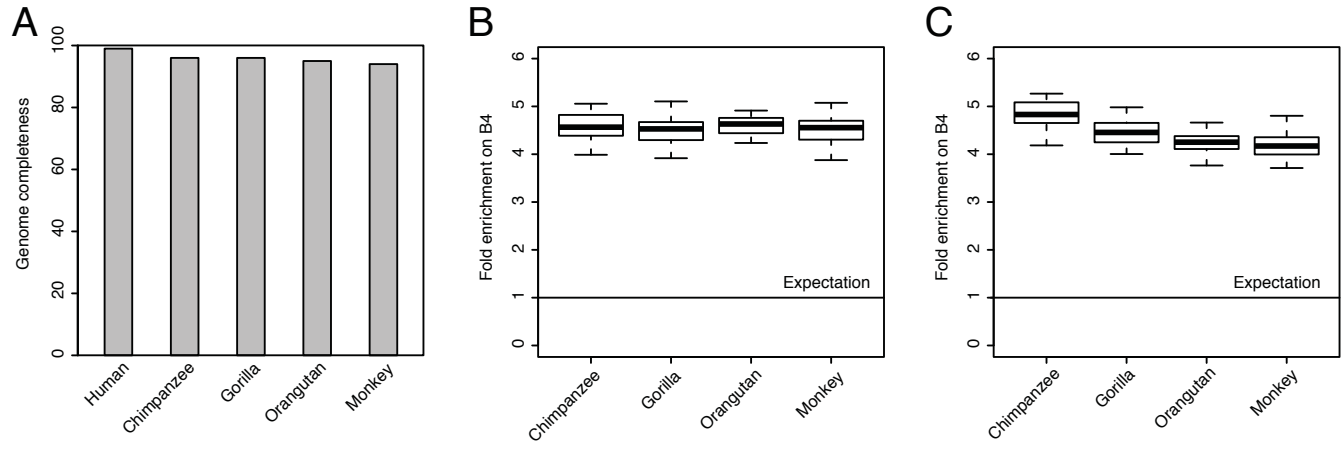


**Figure S1. The effect of genome incompleteness and alignment error on the hEANT evolutionary rate, Related to Figure 1**

(A) Genome incompleteness of different primate species. (B) and (C) The effects of false negative (B) and positive alignment (C) on the acceleration of hEANT evolution. Specifically, we randomly added or removed 10% of the human enhancers aligned to the genome indicated in the x-axis and examined the fold enrichment of EANTS on B4, as shown in Figure 1B. This analysis was repeated 100 times and the results are shown as boxplots. The horizontal line in the box is the median, the bottom and top of the box are the first and third quartiles, and the whiskers extend to 1.5 IQR of the lower quartile and the upper quartile, respectively.

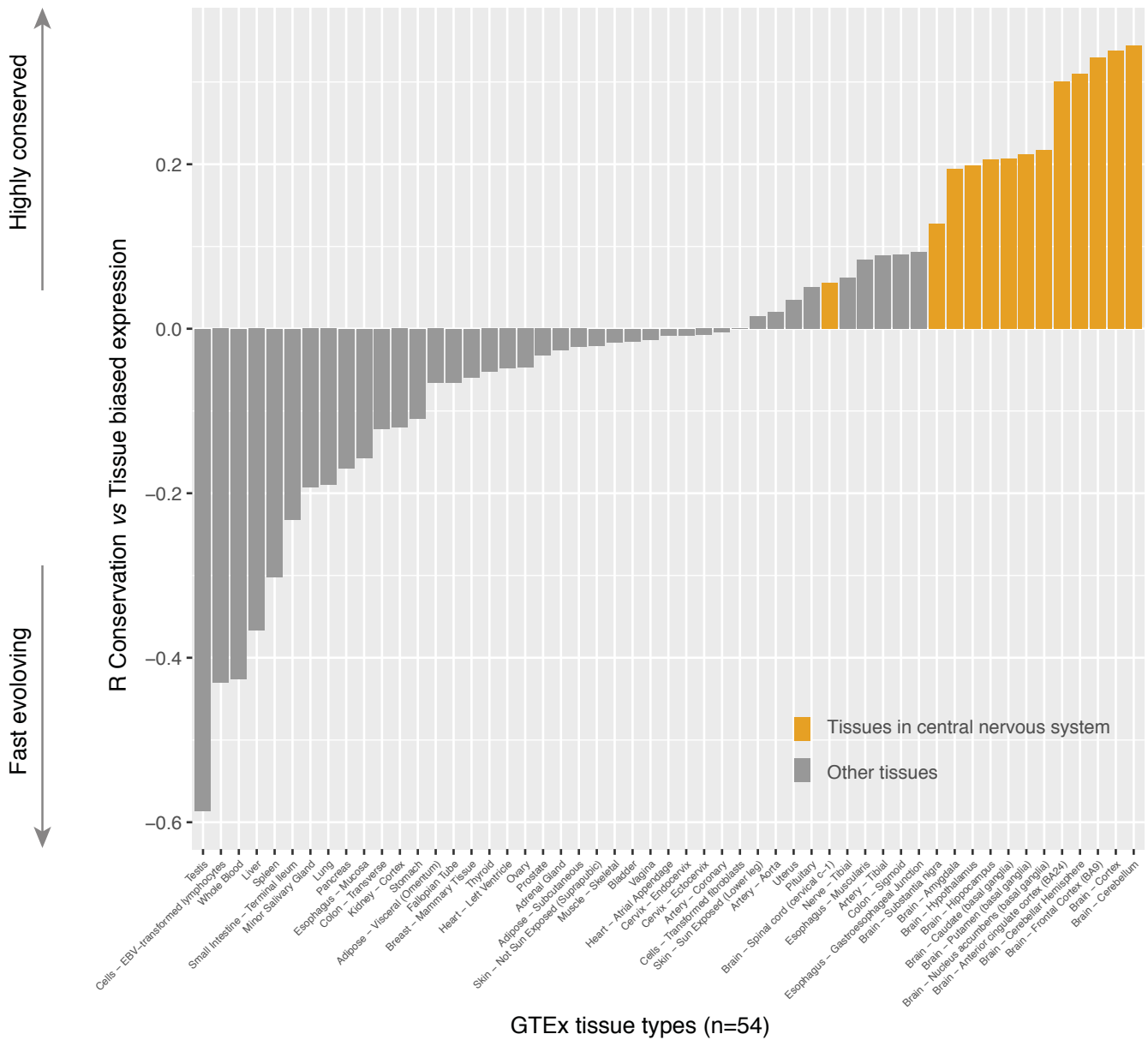


**Figure S2. Conservation analysis on protein-coding genes, Related to Figure 1**

For each of 16,001 protein-coding genes, we determined its conservation level ( $1-dN/dS$ ) and tissue expression bias in the 54 GTEx tissues (STAR Methods). The y-axis shows the correlation (Pearson's R) between gene conservation and expression bias for the tissue type indicated in the x-axis.

**Table S4. TCGA RNA-seq data used in this study, Related to Figure 3**

Cancer type	TCGA abbreviation	Sample size (OS)	Sample size (PFS)
Bladder urothelial carcinoma	BLCA	405	319
Breast invasive carcinoma	BRCA	1,092	1,001
Cervical squamous cell carcinoma and endocervical adenocarcinoma	CESC	303	263
Colon adenocarcinoma / Rectum adenocarcinoma	COAD/READ	616	539
Glioblastoma multiforme	GBM	152	105
Head and neck squamous cell carcinoma	HNSC	517	391
Kidney chromophobe	KICH	64	62
Kidney renal clear cell carcinoma	KIRC	448	358
Kidney renal papillary cell carcinoma	KIRP	288	267
Brain lower grade glioma	LGG	454	NA
Liver hepatocellular carcinoma	LIHC	370	319
Lung adenocarcinoma	LUAD	504	428
Lung squamous cell carcinoma	LUSC	491	371
Ovarian serous cystadenocarcinoma	OV	291	239
Pancreatic adenocarcinoma	PAAD	177	138
Prostate adenocarcinoma	PRAD	374	369
Sarcoma	SARC	258	230
Skin cutaneous melanoma	SKCM	103	89
Stomach adenocarcinoma	STAD	407	323
Testicular germ cell tumors	TGCT	133	131
Thyroid carcinoma	THCA	500	486
Thymoma	THYM	117	113
Uterine corpus endometrial carcinoma	UCEC	316	296
Total	23 cancer types	8,380	6,837

OS is overall survival; PFS is progression-free survival

**Table S5. GWAS supporting the associations between hEANT neighbors and aging-related diseases, Related to Figure 4**

hEANT neighbor	Trait	SNP rs	Chr	Location	Source	PubMed	Analysis ID	Study ID	Study Name
<i>AOAH</i>	Parkinson's disease	17329669	7	36851929	dbGaP	16252231	2842	48	Mayo-Perlegen LEAPS (Linked Efforts to Accelerate Parkinson's Solutions) Collaboration
<i>AOAH</i>	Hypertension	3807609	7	36765758	dbGaP	NA	3042	221	NHLBI Family Heart Study (FamHS)
<i>BMS1</i>	Hypertension	1271546	10	43505098	dbGaP	NA	3041	221	NHLBI Family Heart Study (FamHS)
<i>GAS2</i>	Diabetes mellitus, type 2	7111546	11	22829757	NHGRI	21546767	NA	NA	Genome-wide association scan for survival on dialysis in African Americans with type-2 diabetes
<i>GFRA2</i>	Alzheimer's disease	17581368	8	21662445	NHGRI	21116278	NA	NA	Genome-wide association with MRI atrophy measures as a quantitative trait locus for Alzheimer's disease
<i>KCNK16</i>	Diabetes mellitus, type 2	1535500	6	39284050	NHGRI	22158537	NA	NA	Meta-analysis of genome-wide association studies identifies eight new loci for type-2 diabetes in East Asians
<i>RBFOX1</i>	Alzheimer's disease	17822719	16	6583125	dbGaP	NA	2879	219	GenADA/LONG/Imaging (Genetic Alzheimer's Disease Associations)
<i>SCN2A</i>	Parkinson's disease	764660	2	166213297	dbGaP	NA	2868	89	NINDS Parkinson's Disease
<i>CDH13</i>	Hypertension	11646213	16	82642651	NHGRI	19304780	NA	NA	Genome-wide scan identifies CDH13 as a novel susceptibility locus contributing to blood pressure determination in two European populations
<i>CDH13</i>	Alzheimer's disease	2967391	16	82230392	dbGaP	NA	2879	219	GenADA/LONG/Imaging (Genetic Alzheimer's Disease Associations)
<i>SAMD4A</i>	Parkinson's disease	4901519	14	55019180	dbGaP	NA	2865	126	CIDR: Genome Wide Association Study in Familial Parkinson's Disease (PD)
<i>SLIT2</i>	Osteoporosis	1905843	4	20088059	dbGaP	17903295	1790	7	Genetic correlates of longevity and selected age-related phenotypes: a genome-wide association study in the Framingham Study
<i>TLL1</i>	Osteoporosis	10517865	4	166651016	dbGaP	17903295	1787	7	Genetic correlates of longevity and selected age-related phenotypes: a genome-wide association study in the Framingham Study

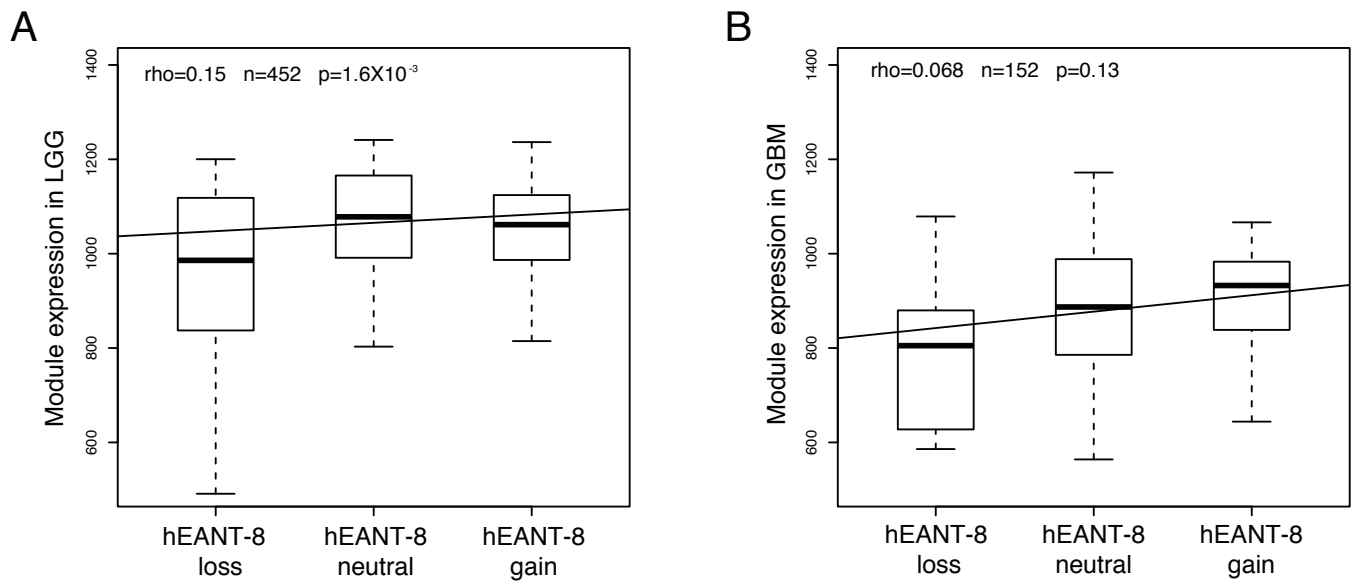


**Figure S3. hEANT-8 is an upstream activator of the co-expression module, Related to Figure 5**

(A) and (B) Module gene expression in different groups of somatic copy number alterations of hEANT-8 (copy number gain or loss) in TCGA LGG dataset (A) and GBM dataset (B). Spearman's correlation coefficient (rho) was used and p value was calculated using Student's t-test. The horizontal line in the box is the median, the bottom and top of the box are the first and third quartiles, and the whiskers extend to 1.5 IQR of the lower quartile and the upper quartile, respectively.

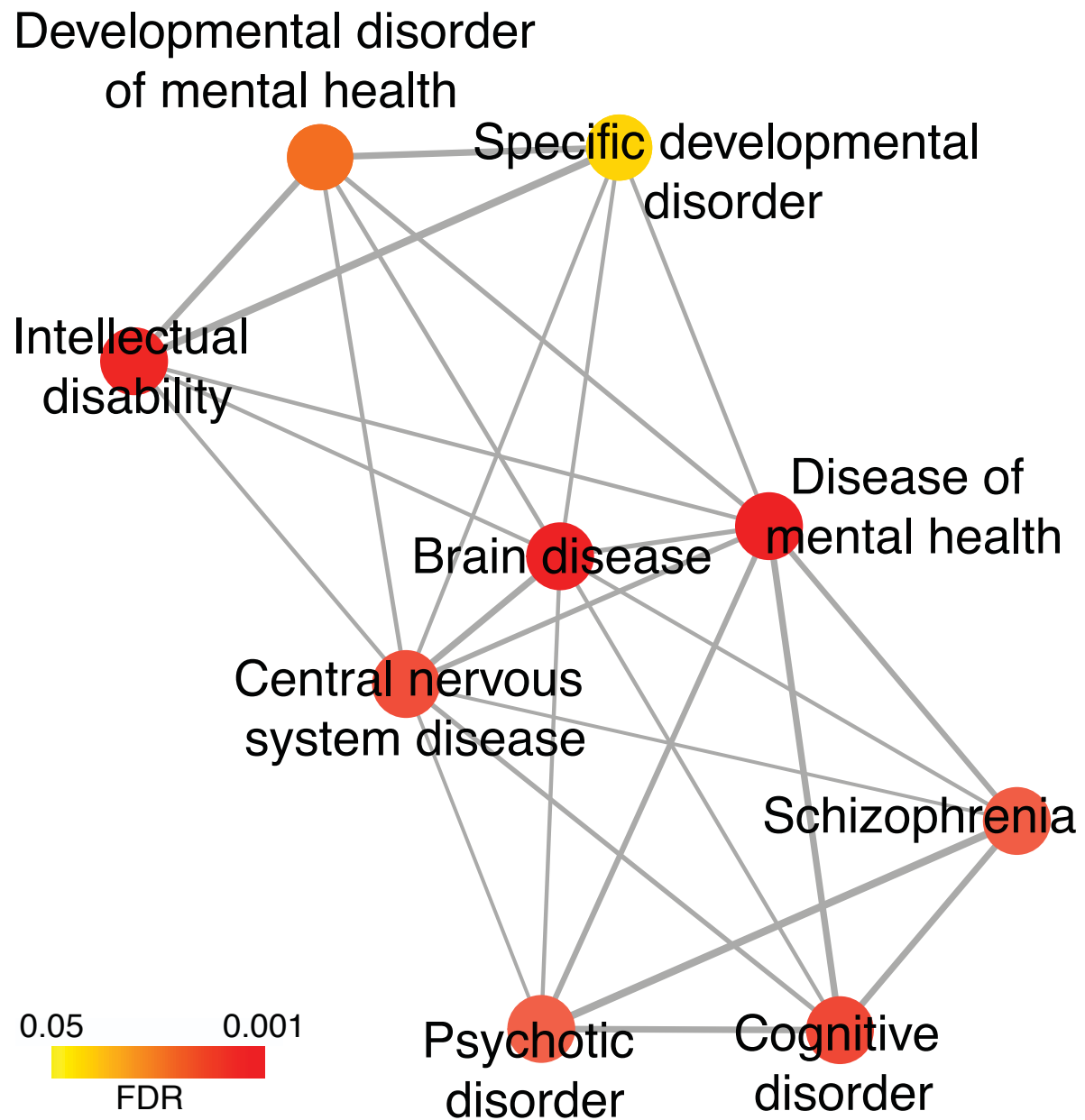


Figure S4. Disease ontology of the hEANT-8 co-expression module, Related to Figure 5

**Table S8. qRT-PCR primers for hEANT-8 coexpression module genes in this study,  
Related to Figure 5**

Gene	Upstream primer	Downstream primer
<i>ACTB</i> (control)	ATTGGCAATGAGCGGTTC	CGTGGATGCCACAGGACT
<i>CDK5R1</i>	TTCACACAGCACCTCCTCTC	ATCCTGTGGATGCAACGTAA
<i>CELF3</i>	AAAGGAGGCTTCCAAGGTTA	CTTAGGGCTTATGCAGTCCA
<i>CHRNBT2</i>	AGTCTGACAGGCAACTGGAG	CCAGGAATGGAATGAAACTG
<i>FAM57B</i>	CAATTGCTGTGCCCTACTT	ATGAGGAACTCCTTGTGCAG
<i>GDAP1L1</i>	GCCGACATCAAGACTCAACT	GAGGGTGTGCTCATGGTATC
<i>GPRIN1</i>	AAGAATGGGCCTGTATCCTC	TTGCTGAAGCCGTAGTATCC
<i>INA</i>	TACAGGAAACTGCTGGAAGG	GTGATAGCCCAGTGGATGAG
<i>KCNIP2</i>	CAAGGAGACTCCAGCACCTA	GGTACGTGTACTTGCCCATC
<i>LICAM</i>	GCCAAAGGAGACAGTGAAGC	GCGTGGCAGATGTAGTCTGA
<i>RUNDCT3A</i>	ACCACCAAGACGGTTCTATGA	TGCGTGAACCTTAGGTAGGG